

## Chapter

# WSN System Warns Producer When Micro-Sprinklers Do Not Work in Fruit Trees

*Federico Hahn Schlam and Fermín Martínez Solís*

## Abstract

Salts in the irrigation water cause micro-sprinklers to clog. Farmers find it difficult to detect sprinkler clog due to the great number of trees grown in commercial orchards, causing a reduction in yield and timing problems. In this article, IoT can support farmers with daily soil moisture detection. A wireless sensor network, WSN was developed to warn the farmer from micro-sprinkling clogging. Trees were gathered into groups of 9 trees, where the central tree holds the master microcontroller and the other eight trees presented slave microcontrollers (nodes). The system uses BLE (Bluetooth Low Energy) to communicate between the master microcontroller by BLE. A second WSN using lasers was also tested but resulted to be a little more expensive. Soil moisture sensor performance against corrosion and current consumption was analyzed being the best sensors the V1.2 capacitance probe and the sprinkler-encoder one. When micro-sprinklers did not apply water to a tree, its number was transmitted via LoRa from the master to the producer's smartphone to warn him/her. A hexacopter was used to detect canopy stress from a height of 30 m, but only after 7 days of water removal did the NDVI indexes detect it.

**Keywords:** BLE, soil sensors, nuts, LoRa, WSN-smartphone, UAV, NDVI

## 1. Introduction

Mexico has planted areas exceeding 44,000 hectares of pecan trees (*Carya illinoensis Koch*) in arid zones [1]. Production of pecan nuts in Mexico affects the United States' nuts prices as 95% of the world production of pecan nuts comes from North America (Mexico and the United States) [2]. Other countries producing pecan nuts are Australia, Israel, and Peru [3]. California plants 350,000 ha of almonds being 77% of the world's production [4, 5]. Almond trees require between 700 and 1500 mm of water to obtain good yields [6] so they need irrigation systems. A high-yield mature almond orchard in South Australia presented evapotranspiration (ET<sub>c</sub>) of 1430 mm [7]. ET<sub>c</sub> used annually by pecan trees in Egypt was 2100 mm [8]. Water use by almond trees depends on canopy cover and evaporative demand [9].

Better irrigation water use efficiency was obtained with pressurized systems than with furrow irrigation [10]. Drip irrigation saves 30% of the water applied

to almond trees when compared with surface irrigation [4, 11]. Almond farms in Australia use high-efficiency drip systems using from 12 to 15 ( $2 \text{ l h}^{-1}$ ) drippers per tree [12]. Pulsing irrigation and deficit irrigation increased water productivity. Less water productivity was increased using deficit irrigation. The modeled water uptake using the HYDRUS-2D software was higher than sap flow measurements before the almond harvest [12]. Sprinkler irrigation systems in pecan trees produced greater trunk growth diameter in contrast to other irrigation systems [13]. Wet soil volume from micro-sprinklers was important for almond yield [14]. Sustained deficit irrigation applied water at a given percentage of full  $ET_c$  over the entire season and provided excellent yield [15].

Automatic irrigation systems require sensors to log irrigation variables [10]. Fruit trees are sensitive to water deficit, so irrigation evaluation becomes critical. Water stress monitoring during deficit irrigation allows saving water without decreasing fruit yield [16]. For fruit trees, monitoring the control of soil moisture is important to avoid the proliferation of fungi in the roots under high levels of humidity [17]. Tensiometers measure soil water potential and are useful for timing irrigations [18]. Continuous monitoring with dendrometers is time-consuming and problematic for automated irrigation [19]. Midday stem water potential (MSWP) has thus become the current standard irrigation management tool [20].

LoRaWAN radio signals within forests can be attenuated due to diffraction and scattering effects caused by tree obstacles [21–23]. Low frequencies provide good penetration within forests and present lower losses than high-frequency bands [24]. Tropical orchards can experiment with drastic weather conditions, being air temperature the variable that affects more LoRa transmission [25–27]. Air temperature decreases the received signal strength indicator (RSSI) variable [25]. Rain and relative humidity did not affect RSSI strongly [25, 28].

Precision agriculture in fruit crops has become fundamental for optimizing yields [29]. Internet of Things (IoT) has been used in recent years for plant growth monitoring [30]. Unmanned aerial vehicles (UAV) can observe trees that cover several hectares with multi-spectral cameras [31]. Normalized difference green near-infrared index (NDGNI) obtained with spectral cameras has also proved to be sensitive to water status [32]. Multispectral imagery remote sensing can monitor crop ET and crop water use throughout the growing season [33]. The normalized difference vegetation index provides a reliable estimate for leaf chlorophyll content and LAI [34]. The B5:B7 near-infrared ratio positively correlates with the moisture status of pecan orchards [35].

In this chapter, sensors detect when the micro-splinker system is not irrigating trees properly. The proposed remote monitoring network is able to: (1) monitor soil moisture in each tree of the orchard at sunset; (2) trigger an alarm if soil moisture was not detected; and (3) warn the producer by sending a short message system (SMS) to his/her smartphone. The WSN (wireless system network) for different moisture sensors and orchard densities are reviewed.

## **2. Walnut tree orchard**

The experiment during the 2018–2019 season was carried out in the Western walnut-tree plantation at Delicias, Chihuahua, Mexico ( $28^{\circ}11'35'' \text{ N}$ ,  $-105^{\circ}28'18'' \text{ W}$ , 1190 m). The 25-year-old orchard has a density of  $10 \times 10$  trees per hectare with an average tree height of 7 m. Four micro-sprinklers were added per tree, together with

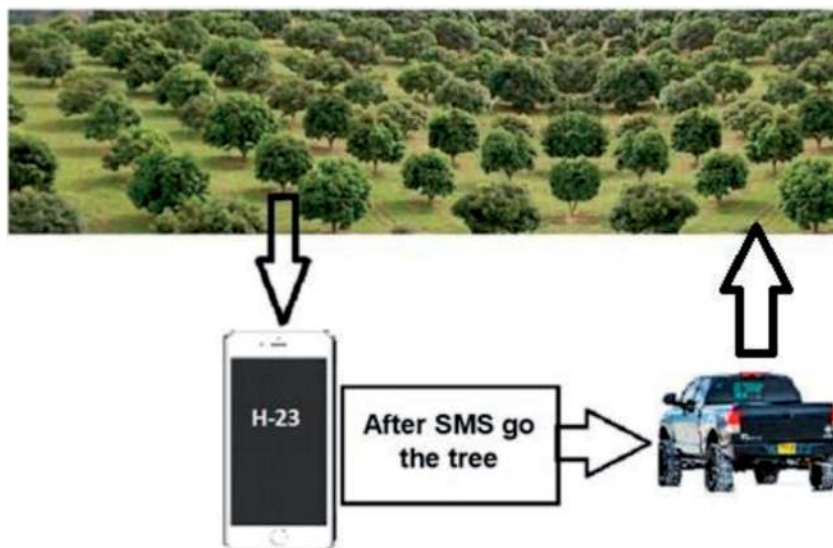


**Figure 1.** Orchard monitoring provides a smartphone message to target the tree where irrigation problems were detected.

a water moisture sensor. Once the farmer receives a smartphone message (SMS) containing the tree number where irrigation failed, he/she drives to the tree and cleans the micro-sprinkler, letting it ready for the next irrigation cycle (**Figure 1**).

Tree number per hectare characterizes orchard density, which is important to increase yield. Almond tree size and height increase with age, and in order to obtain good yield, it is necessary to prune the orchard and let the radiation pass through the canopy. The reduced yield was obtained in almond low density (LD) farms with compost application [36]. Super high-density (SHD) orchards (over 2000 trees/ha) were studied since 2010 [37]. Kernel and almond in shell yield were 1.58 and 4.43 ton/ha, respectively [37]. The 25-year-old Western walnut-tree plantation in Delicias, Mexico, with a density of  $10 \times 10$  trees per hectare, sprinkler irrigation, and a nitrogen application of 200 kg/ha produced 33 kg/tree [38]. Tree crowding reduces productivity due to excessive shading [39]. Tree management, including spraying and harvesting, becomes more difficult.

## 2.1 Soil and tree water content detector

Real-time monitoring of the whole orchard is impossible to carry out without sensors. Each tree presents a monitoring system consisting of moisture sensors, a microcontroller, and some of them a master microcontroller with a LoRa transmitter (TTGO LoRa32 OLED V2.1.6., Lilygo, China). A plastic box in each tree trunk covers a low power consumption CC2541 chip inside (**Figure 2**). The CC2541 built by Texas Instruments includes a Bluetooth Low Energy (BLE) platform, a built-in 8051 microcontroller, 256 KB of programmable memory, 8 KB of RAM, IO ports, and a 2.4-GHz RF transceiver.

### 2.1.1 Soil moisture detectors

Precise soil moisture measurements can be obtained with the gravimetric method, using tensiometers, neutron gauges, gamma-ray attenuation, and time-domain

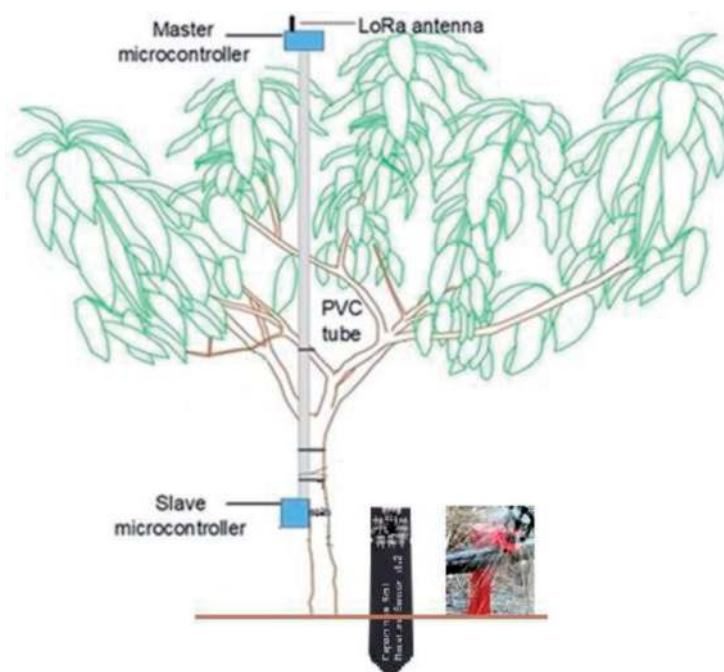


**Figure 2.**  
*Tree controller and transmitters.*

reflectometry (TDR) [40]. Neutron probes, TDR, and gamma-ray sensors are highly accurate but extremely expensive. The neutron probe costs around \$10,000 and estimates water in a larger area than other soil moisture sensors. TDR needs a very good data logger (\$2000–3000) and each sensor cost is 100 US\$.

Traditional farming depends on farmers’ skills and experience. A transition to smart farming is noticed in advanced countries. Smart farming optimizes yields after measuring environmental and crop conditions. Soil moisture measured at multiple locations requires cheap sensors. Low-cost dielectric soil moisture sensors require complex processing circuits and are dependent on soil type and temperature [41]. Five different soil moisture sensors are compared in **Table 1** [17, 42], and prices are decreasing as smart technologies take over. The Decagon EC-5 sensor measures volumetric water content (VWC) after obtaining the dielectric constant by frequency

Model	Type	Sensit, %	VCD	Size mm	Cost \$	Ref
MT-02A	Cap	3% 0–53 5% 53–100	3.6–30	149 × 45	79	[17]
YL-69	Res	0–95	3.3–5	60 × 30	2.6	[17]
Wat-200 s	Res	0–95	4–15	100 × 50	50	[42]
Theta Probe	Refr	xxxx	5–14	158 × 40	998	[43]
DecE-05	Diel	0–100	2.5–4	89 × 18	105	[42]
VH400	Diel	0–95	3.5–20	95 × 7	40	[42]

**Table 1.**  
*Comparison of relatively cheap soil moisture sensors.*

domain technology [42]. As the sensor works above 70 MHz, its cost increases to 105 US\$, due to all the electronics involved, **Table 1**. It works accurately in soilless media and under saline soils.

Remote dielectric and capacitive soil water content sensors are becoming attractive as the Delta-T ThetaProbe is being precise but very expensive [43]. The YL-69 soil moisture sensor [17] provides a variable electric signal when water is present between the electrodes and the soil. Ion movement in wet soil is higher than in dry soil. This sensor is equipped with an LM393 potentiometer and provides a digital output depending on the soil moisture [44]. Clay and loamy soil samples will provide different YL69 output values when the soil has a different moisture content [45]. Clay and loam soil with 20% moisture will obtain sensor measurements of 90 and 70%, respectively. In clay soils, sensor readings are linear only until 13% [45].

### 2.1.2 Cheap soil moisture measurements

In this experiment, several moisture sensors were used to compare efficiency, energy consumption, and cost.

- Capacitive V1.2 sensor: This soil moisture sensor (Paialu, China) is buried 6 cm and requires a DC voltage of 3.3 V (**Figure 3a**). The output is connected to a CC2541 microcontroller. This sensor is not affected by corrosion and its output should be close to 500 under dry conditions in clay and loam soils and 420 under wet conditions. This output is the one provided by the CC2541 microcontroller.
- Resistive YL-69 sensor: This sensor is smaller than the V1.2, so it is only buried at 5 cm. A potentiometric module YL-38 (**Figure 3b**) can be added to provide a digital output when it arrives at a given soil moisture threshold. The probe is calibrated using the air and water as dry and 100% humid values, respectively. Once buried in the soil (**Figure 3c**), it will not require further calibration.
- Wetness sensor: The PCB circuit board is composed of several cooper thin wires. Its resistance changes when water is sprayed (**Figure 4a**). The resistance reaches a maximum of 200 k $\Omega$  when the air is dry and 5 k $\Omega$  when air is moistened by sprinkler irrigation. Drops generally remain over the PCB board for some minutes.

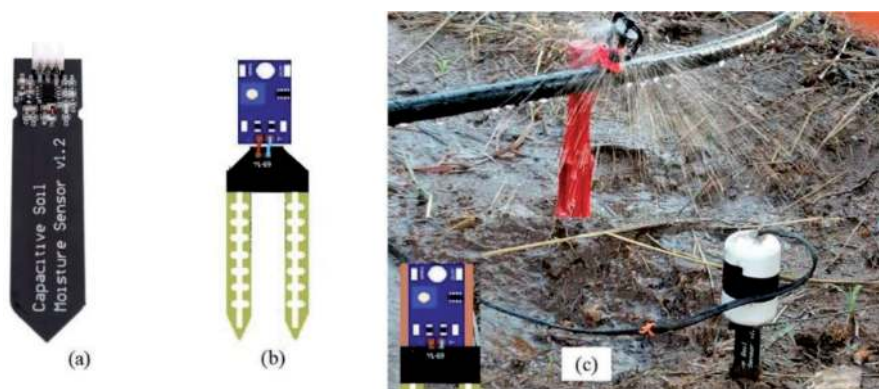


**Figure 3.** Moisture (a) capacitive V1.2 probe, (b) YL-69 probe, and (c) V1.2 and YL-69 probes buried in soil.



**Figure 4.** Sprayed water (a) to a wetness sensor, (b) to a dry solar cell, and (c) to forming drops in solar cell.

- Solar cell sensor: The 5-watt panel (**Figure 4b**) can be used to charge a capacitor. When the solar panel gets wet (**Figure 4c**), no charge will be supplied to the capacitor. Once the detection is carried out at sunset the capacitor is discharged.
- Sprinkler rotation sensor: This sensor detects whether water is being applied. As the micro-sprinkler starts operating, a circular washer on its top surface rotates. This washer presents one small orifice that rotates. A high-performance, low-cost, optical incremental encoder module (mod HEDS-973x, Avago Technologies, USA) counts the number of pulses and charges a capacitor during irrigation (**Figure 5a**). Ambient temperature can increase over 70°C and its voltage supply can work from 0.5 to 7 VDC.
- Air temperature and humidity sensor: The DHT11 is a low-cost digital sensor. It uses a capacitive humidity sensor but new data can only be acquired every 2 s. Humidity can be read from 20 to 80% and its energy consumption is of 2.5 mA per reading. It is recommended to hang it from the tree (**Figure 5b**) rather than from the hose, where drops begin to move toward the sensor and can damage it (**Figure 5c**).

## 2.2 Wireless system network

A wireless system network (WSN) monitored water application to each tree within one hectare. Every tree group consists of 9 trees (**Figure 6**). One hectare is regrouped into 12-groups, being water content detectors monitored at sunset. The central tree (A) from each group holds a master microcontroller module (TTGO LoRa32 OLED V2.1.6., Lilygo, China). This master module is fixed at a height of 5 m at the end of a hydraulic PVC tube (**Figure 2**). The remaining eight trees have CC2541-slave microcontrollers (SM).

The CC2541 uses BLE (Bluetooth Low Energy) for communication taking place at sunset. Once the slave microcontroller receives the packet from the slave transmitter, it responds. If there is no data to send, an empty packet is sent, finishing the BLE connection.

The first group array (**Figure 6a**) communicates via BLE sending a value at 18:00, just at sunset. A sensor detects if water did not reach a tree, so after CC2541 acquisition and processing, it will transmit the tree number to the following tree via BLE. The sequence starts with tree G, transmitting the tree number or 0 to tree E. Tree E detects whether it was irrigated, otherwise it transmits the tree number to tree H.

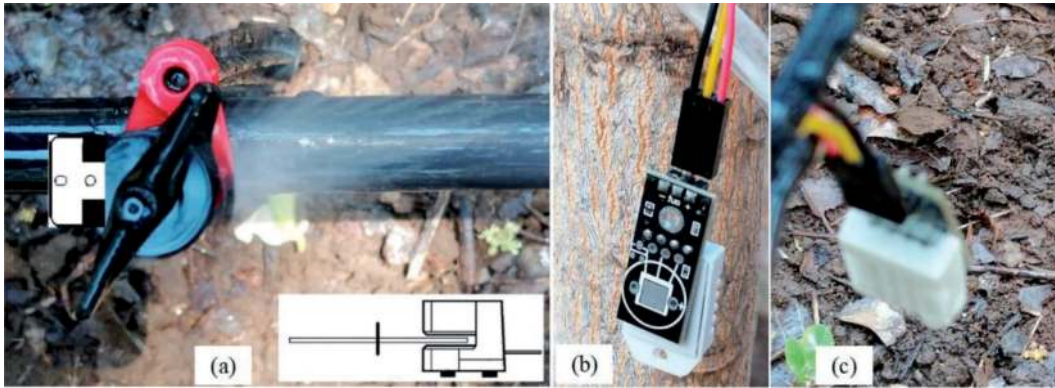


**Figure 5.** Water measurement from (a) a micro-sprinkler with an optical sensor, (b) air moisture sensor DHT 11 hanging from the tree, and (c) DHT 11 hanging from lateral hose.

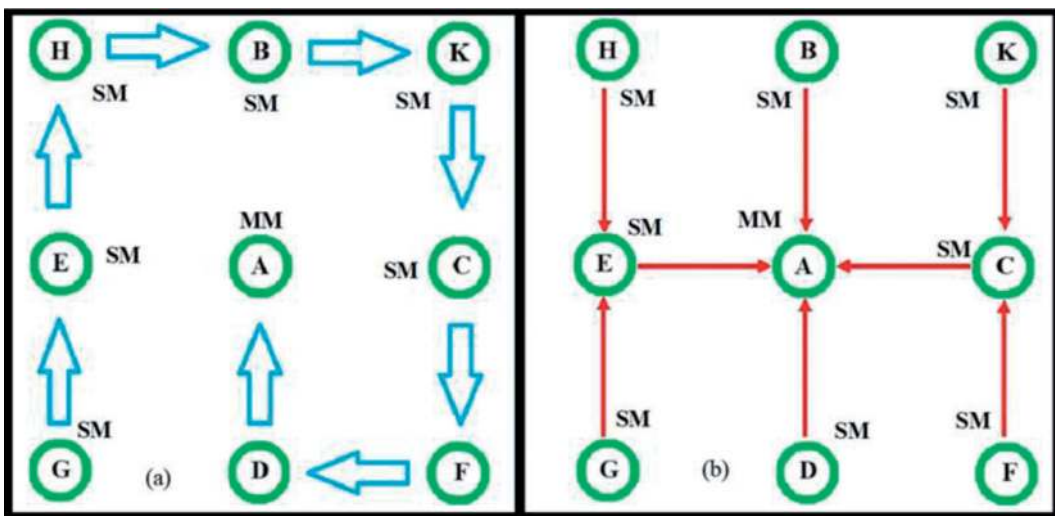


**Figure 6.** Group of 9 trees using (a) BLE transmitters and (b) lasers for the orchard WSN.

This process continues until all the collateral trees send their information reaching the final value to the central tree. The values that will be sent to the producer’s smart-phone by the master microcontroller LoRa vary depending on the number of trees that were not irrigated. Trees are numbered from 1 to 108 in 1 ha, so the third group has trees numbered between 19 and 27. If G, E, and H failed due to a lateral problem, the data received by the master microcontroller will be 212,019 (**Figure 7a**). If only E and C trees were not watered, the data that will be arriving to the master is 2026 (**Figure 7a**). If all trees were watered, no data reaches the microcontroller.

Another group array topology (**Figure 6b**) substitutes the BLE signal with optical lasers. A CC2541-slave microcontroller (SM) was placed in each tree surrounding the central tree (A). The master microcontroller (MM) at tree A is the TTGO LoRa32 OLED V2.1.6. Each CC2541 reads the sensor signal, determines whether the tree soil is dry, and turns on the laser in case the tree soil is dry. A battery charged by a solar panel supplies the energy required to turn on the 650 nm–5 mW laser diode (D650-5I, USLASERS INC, USA). The phototransistor at the adjacent tree (10 m away) saturates after being lighted by a laser beam with a 14 mm diameter. A capacitor charges and

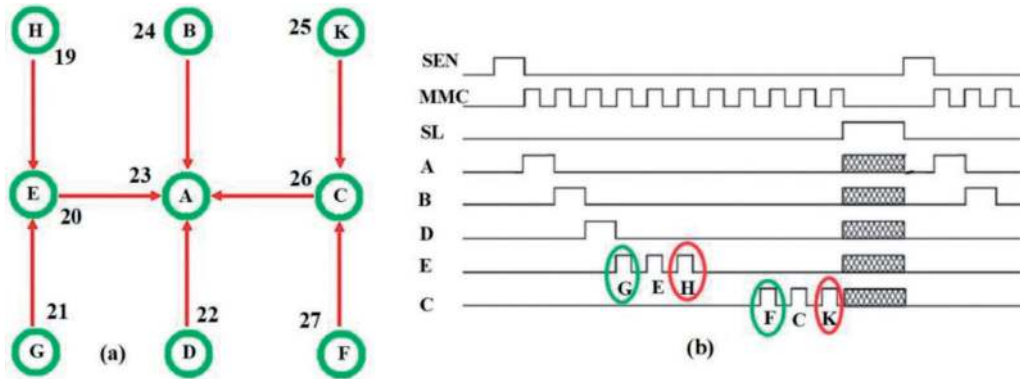


**Figure 7.** Third group of 9 trees (a) using BLE lasers for WSN and (b) master microcontroller signals.

this voltage will be read by the CC2541. The phototransistor (BPW76A, Vishay, India) was chosen as it operates under a wide temperature range using an operating voltage up to 5 V and a collector current of 0.5 mA.

As lasers do not transmit electrical signals, the CC2541 turns on the laser providing a 1.5 s pulse. The CC2541 slave microcontroller on tree E acknowledges its own water status, before checking if the capacitors were charged by lasers from trees H and G. If no charge is detected and the tree was watered, the CC2541 goes to sleep (**Figure 6b**). Tree A will hold 4 phototransistors to acknowledge the moisture status of the entire group. The master microcontroller timing signal explains its operation, being synchronized by the microcontroller clock (**Figure 7b**).

A light sensor indicates when sunset arrives, starting the operation routine. Once the MM is operating, it acquires the tree A sensor value first and waits 3 s for checking the capacitor status. It will charge through the phototransistor if tree B laser beam is on. If this is the case, it saves number 24 in a register (**Figure 7a**). The same operation takes place with tree D (number 22) 3 s later.

Information coming from trees E and C has to be decoded. It also contains information from trees H and G, and K and F. Laser from tree E sends 3-pulses of 1.5 s each, separated by OFF pulses of 1.5 s. The three pulses sent by the CC2541 controller are shown at the E timing signal (**Figure 7b**). Three pulses are sent, when trees G, E, and H were not watered. If only the first pulse appears (green pulse), tree G is not watered and the master microcontroller will convert it to number 21 (**Figure 7a**). The same operation takes place with tree C. After checking all the trees, the MM generates a value that is transmitted through LoRa, and the tree enters sleep mode until the next day.

### 2.2.1 Master LoRa communication

LoRa provides a low-cost communication system that does not require a license. TTGO LoRa32 OLED V2.1.6. modules can communicate through BLE and LoRa. The LoRa was programmed at 915 MHz, with a power transmission of 20 dBm, a spreading factor (SF) of 12 and a bandwidth of 125 kHz. The maximum packet size for a 9-tree group would be 18 bytes if all the trees were not watered at the same time.

Another TTGO LoRa32 OLED V2.1.6 module at the roof of the farmer's house works as a general receiver from the entire plantation and presents a 3 dBi 915 MHz whip antenna. In addition, a SIM Card is incorporated so that the tree number with water shortage could be transferred to the farmer's smartphone by SMS.

Transmission between the 12 central tree modules within a hectare and the end TTGO LoRa32 OLED V2.1.6 module at the orchard house was synchronized to avoid crossover between SMS messages. The time delay for this transmission takes 13 s. The 3 central trees further away transmitted their data 1–2-min after sunset. LoRa from the following 3 groups transmitted data 3–4 min after sunset and so on.

### 2.3 Optical remote sensing measurements

In situ soil moisture monitoring of crop water stress is time-consuming, and assumes uniform plant density and transpiration rate [46]. Vis–NIR (400–1100 nm) can provide measurements of soil moisture [47]. Hydration, hygroscopic, and free water are present in the soil, being the free water inside soil pores. Spectral absorption peaks for hygroscopic and free water occur at 1900 nm but cannot be measured with a cheap VIS–NIR spectrometer. Vis–NIR optical soil moisture measurements require large local calibration data sets limiting their use [48]. Remote sensing detects vegetation stress in trees [49, 50], but satellites provide low-resolution images with a limited field of view. Nano-satellites increase spatial resolution and image timing [50]. NDVI (Normalized Difference Vegetation Index) [51] and crop water stress index [49, 52] have been correlated against canopy temperature and tree stress. NDVI provides useful information on canopy structure and drought stress [53].

#### 2.3.1 UAV selection and flight programming

A six-wing DJI S900 (DJI Co., Ltd. Shenzhen, China) with a load capacity of 5 kg was selected to take tree images (**Figure 8a**). Time of flight at midday took 18 min and was done at a height of 30 m at a speed of 4 km h<sup>-1</sup>. Multi-rotor drones used to study pistachio, almond and walnut plantations collect RGB, and multi spectral images [54]. The hexacopter was equipped with a Parrot Sequoia multispectral camera (SenseFly, Inc., Switzerland). The Parrot equipment presents 2 sensors: a

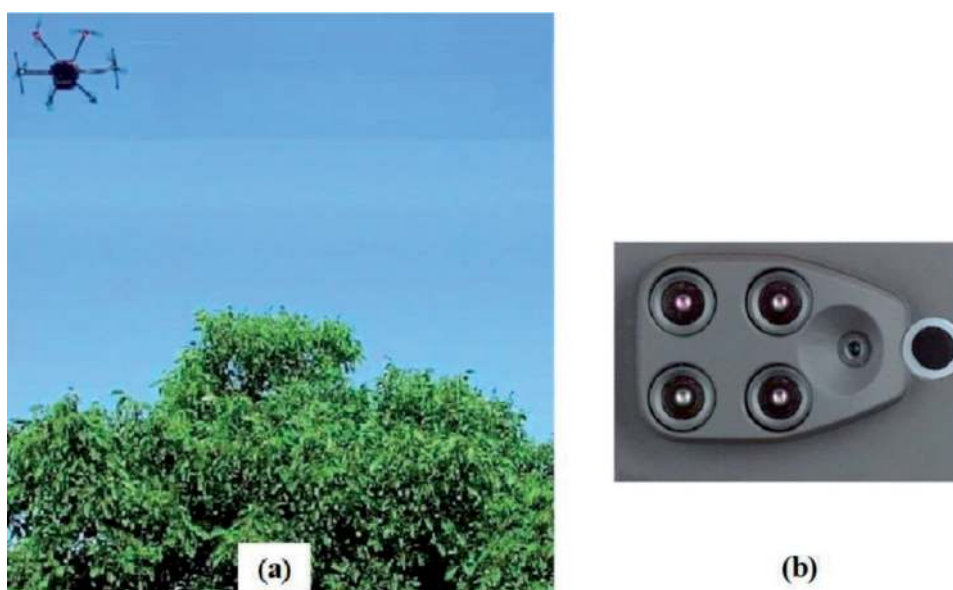


**Figure 8.**  
*Hexacopter (a) flying over tree and (b) parrot camera.*

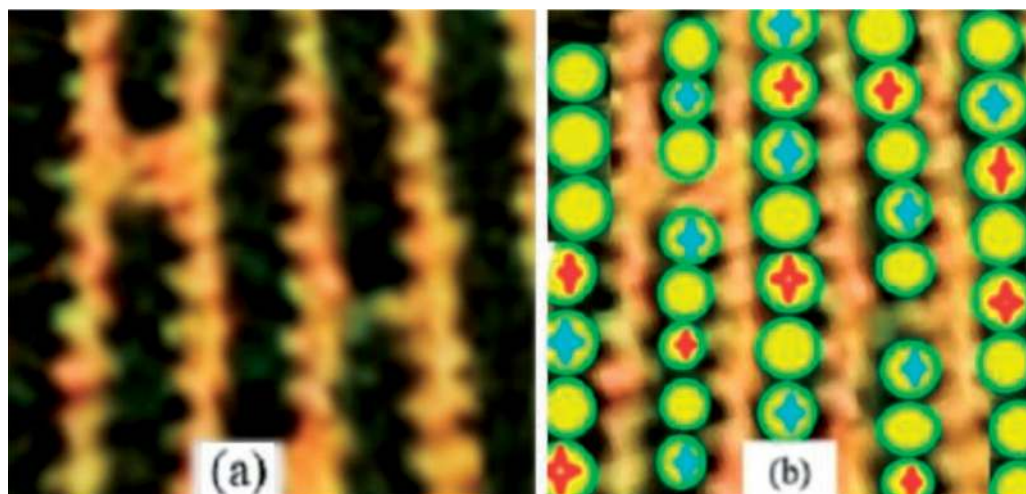


**Figure 9.** Image taken by the hexacopter (a) in RGB and (b) showing trees with sprinklers removed.

multispectral camera and a light sensor to monitor sunlight intensity. The multispectral sensor has four (1.2 megapixels) monochrome cameras: green, red, red edge, near-infrared, and 16 MP RGB[55]. Their RGB and multispectral spatial resolution were of 1.2 cm/px and 3.8 cm/x, respectively [56]. The hexacopter took aerial images of the plantation on the day when some micro-sprinklers were removed as well as 4 and 7 days after (**Figure 9a**). Aerial images were taken every 2 s, having an overlap of 80%. Some trees had all their 4 micro-sprinklers removed (red cross), meanwhile those trees with a blue cross had only one sprinkler removed (**Figure 9b**). The experiment was repeated 3 times. After the UAV returned, images were exported for processing with Pix4D software (Pix4D v.3.1., Switzerland).

### 3. Results and discussion

The results obtained can determine the best cheap sensors for sensing if the micro-sprinklers applied water in the orchard, being a useful precise agriculture application. Transmission effects due to laser, BLE, and LoRa are all considered. UAV data were analyzed to obtain the NDVI index to determine if sprinkler application can be detected remotely.

#### 3.1 Sensor experimental comparison

A general comparison of the sensors used within the plantation is shown in **Table 2**. The first two sensors (capacitive V1.2 and YL-69 probes) were tested in sixty trees studying their performance during the month of April (**Figure 10a and b**). When soil moisture increases, the conductivity of soil rises and the YL-69 values vary between 400 and 650 (**Figure 10b**). These values result from the 10-bit ADC (analog-digital conversion) carried out by the CC2541 microcontroller. The sensor analog output provides moisture levels that will be converted to a digital signal that varies between 0 and 1023.

Dry clay and loam soil monitored with YL-69 probes presented average ADC values of 503 and 640, respectively. Their standard deviations were 28 and 22,

Model	Sensitivity %	Efficiency	Current, mA	Wireless system	Cost \$
V 1.2 sensor	3–95	100	5	A, B	2.8
YL-69 sensor	0–95	100	5	A	2.65
Wetness PHY31	0–95	78	3	B	65
NORPS-12	0–95	82; 35	0.47	B	1.8
Sprinkler encoder	0–100	100	5	A, B	7
DH11 sensor	0–95	100	2.5	B	2.4

A: BLE system (Figure 6a); B: laser system (Figure 6b).

**Table 2.**  
 Comparison of sensors for detecting micro sprinkler application.

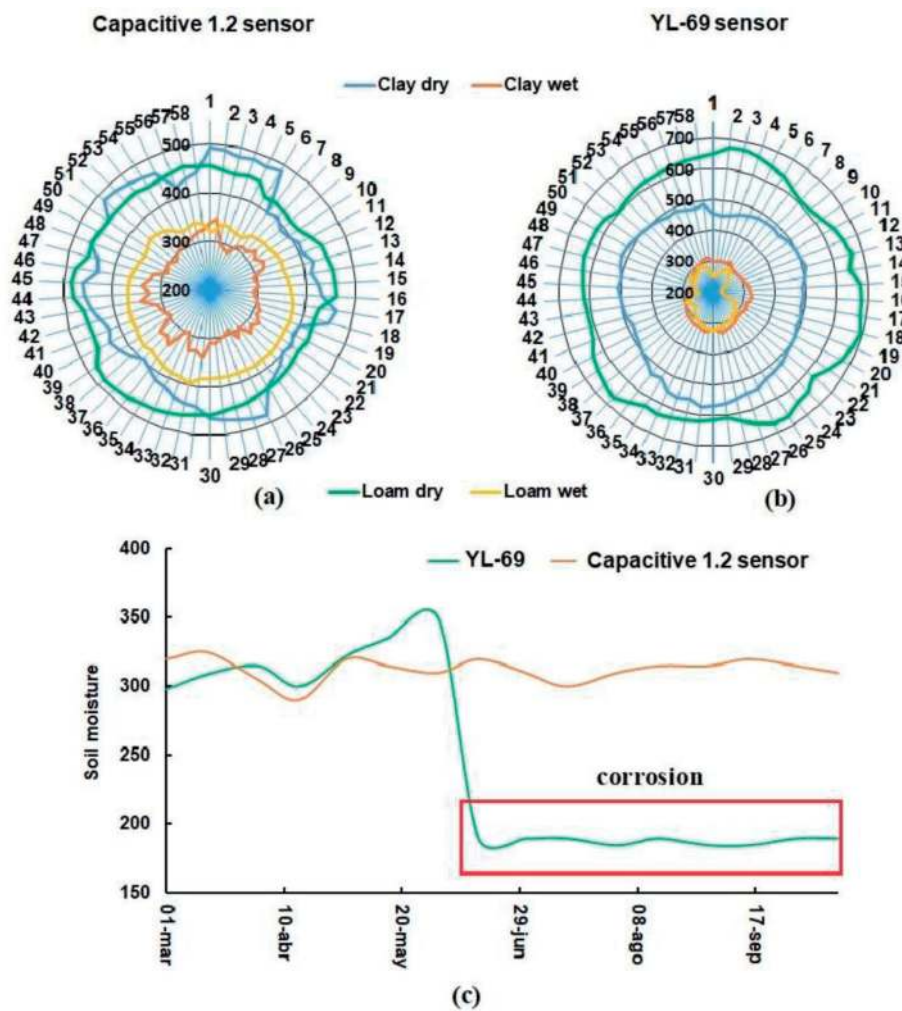


**Figure 10.**  
 Measurements of (a) 60 capacitive 1.2 sensors, (b) 60 YL-69 sensors for dry and wet soils, and (c) both probes during a period of 6 months.

respectively. After micro-sprinkler irrigation, soil moisture increased at least by 50%. YL-69 average measurements in clay and loam decreased to 307 and 276, respectively. Their standard deviations were 15.21 and 26.9, respectively. The variable resistance

YL-69 probe's maximum wet value for both soils was 338 and the minimum dry value was 449 in clay soil, being easy to discriminate.

A similar study carried out by Adla et al. [57] provided excellent results for monitoring soil moisture in all kinds of soils including those with sand. Soil resistivity is influenced by salt concentration in water [58] or by salts added as fertilizers. A sensor was left in the soil nearby the tree and it did not respond after 3 months (**Figure 10c**). YL-69 probes coated with nickel plating rusted after 4 days requiring replacement [59].

The capacitive 1.2 sensor is a cheaper version of the SM100 Soil Moisture sensor built by Spectrum Technologies [57]. In dry clay and loam soil, average moisture was similar being 442 and 455, respectively. Wet average soil clay and loam moisture values were 316 and 367, respectively. Their standard deviations were 16.4 and 17.3, respectively. Minimum dry clay soil measurement was 396, meanwhile maximum wet soil measurement in clay was 361. A 100% discrimination was obtained as noted by the blue and orange lines of **Figure 10a**. Dry and wet soil was also perfectly discriminated in loam soils (**Figure 10a**). Sensors made of a corrosion-resistant material monitored wet clay soil for 8 months, varying between 280 and 330 (**Figure 10c**). These sensors supplied by AC (alternating current) do not rust, resulting in longer operating life.

The solar cell sensor (**Table 2**) provides an extremely small current due to the short operation time and poor illumination intensity at dusk. The solar cell was substituted by a light-dependent resistance (LDR) that measures illumination. The selected LDR (mod. NORPS-12, Silonex, the UK) is encapsulated with a humidity-resistant coating. The resistance of the LDR is 6 k $\Omega$  when it is illuminated by a LED and increases to 1 M $\Omega$  during dusk. A battery of 3.3 V supplies voltage to a serial divider formed by a 1 k $\Omega$  resistance and the LDR. As the sprinkler deposits water drops over the LDR surface, LED incoming radiation gets scattered within the water. A voltage of 2.83 V is obtained at the divider pin when the LED illuminates the dry LDR surface. With water drops over the LDR surface, the voltage increases to 3.29 V at the divider. The experiment was carried out with one hundred sensors, its efficiency being 83% and 35%, during calm and windy days, respectively. The wind does not allow the drops to stay over the LDR. On calm days, erroneous LDR measurements were found when the sensor slope increased as water drops fell to the soil.

Leaf wetness duration (LWD) sensors provide important information for the prediction of plant disease [60]. Capacitive leaf wetness sensors have been developed for IoT applications with Arduino but their cost is relatively high (48 US\$). When it operates at a frequency of 1 kHz, the sensor responds in 5 s [61]. Leaf wetness sensors (LWS) built, nowadays, on flexible substrates can detect whether the leaf canopy is dry or wet [61]. As water appears over the surface substrate, the dielectric increases.

The Phytos 31 LWS (4 × 6 cm) produces a variable linear voltage according to the surface covered by the water. The sensor was tested around the plantation in different trees to study its efficiency for detecting sprinkler spraying. With the dry sensor, the CC2541 should acquire a value beneath 0.4 mV and when 40% of the LWS area is humid, the voltage provided by the sensor should be over 0.48 mV. Each tree having an LWS was sensed fifteen times during the irrigation period and the average value was saved. After 15 min, the probability to get more drops over the sensor was higher. The efficiency for detecting sprinkler operation was 78%, being dependent on wind, sensor slope, and proper positioning of the irrigation sprinkler. Grasshoppers and spiders were also attracted by the Phytos 31 LWS.

The most innovative system to detect water leaving the sprinkler is to use a C-shaped emitter/detector module. Coupled with a washer fixed to the sprinkler, it

translates rotary movement into a digital output. This was achieved with a HEDS-973X circuit from Avago Technologies. When water is supplied, the sprinkler turns the washer that has a small orifice in it. As light from the emitter diode passes through the orifice, it generates a pulse. The pulse interrupts the CC2541, and after 10 interruptions it will recognize that water was applied. This system worked with 100% accuracy and was not dependent on environmental conditions.

DHT 11 showed extreme variations during the first day of analysis and most sensors got damaged after getting wet for 3 days with saturated water. They were substituted in some trees by the DHT 22 that theoretically withstands 100% RH but also failed after 1 week. The DTH40 (Sensirion, Switzerland) can measure from 0 to 100% RH and it can do it every 8 s. Its energy consumption is 28  $\mu$ A and its cost is 2.87 US\$, but still has to be tested in the field.

### 3.2 Best sensors and current consumption

Section 3.1 compared each sensor and only the capacitance V1.2 moisture sensor and the C-emitter/detector adapted to the sprinkler passed the requirements for great extensions due to their reduced cost and efficiency. These sensors work properly under natural environmental conditions and present high detection accuracy. Sensor current consumption depends on current demand and time of operation per day. For the capacitance sensor, it will take 5 s to measure the soil moisture content. In this interval, several samples are obtained and averaged, consuming 25 mAs per day. The sensor adapted to the sprinkler takes only 1 s to measure. Once this time is multiplied by the 5 mA current used (**Table 3**), it provides the current consumption per day (5 mAs). The costs per hectare for both type of detectors change, needing 400 sensors each. With 400 capacitive V1.2 probes connected to 100-CC2541 controllers, the cost will be 1760 US\$ per hectare. Four hundred sprinkler-encoder sensors connected to one hundred CC2541 microcontrollers inside 1 ha will become more expensive: 4000 US\$.

### 3.3 WSN transmission

Energy consumption of nodes within the BLE (A) and BLE-laser WSN systems are compared in **Table 3**. Current consumption by each node (tree) depends on the sensor used, CC2541 acquisition and processing, and finally transmission current. The CC2541 microcontroller employs 3 and 18.2 mA for each acquisition and transmission/reception, respectively. For the BLE WSN (A) with the soil capacitor sensor V1.2, it will consume ( $25 + 3 + 18.2 = 46.2$ ) mA per day. In the case of the laser WSN, each laser needs 20 mA per second. The CC2541 of trees E and C (**Figure 7a**) turn on the laser 3 times

Sensor/WSN	Sensor, mA	Acq and Proc, mA	Trans/receipt, mA	Total energy, mA day <sup>-1</sup>
V 1.2/A	25	3	18.2	46.2
V 1.2/B	25	3	90	118
Sprinkler A	5	1.5	18.2	24.7
Sprinkler B	5	1.5	90	96.5

A: BLE system (**Figure 6a**); B: laser system (**Figure 6b**); Acq and Proc: acquisition and processing.

**Table 3.**  
 Comparison of sensor nodes for detecting micro sprinkler application.

(1.5 s pulses) when no water is applied by the micro-sprinklers. If 20 mA is supplied to the laser, it will consume 90 mA per day in 4.5 s. All the other trees will consume 30 mA per day during laser communication if water fails. The sprinkler sensor provides pulses to interrupt the CC2541, so lower power consumption of 1.5 mA is required. The node that performs better from an energy point of view is the one having the sprinkler sensor and transmits the data through CC2541 BLE controller (**Table 3**); it only employs 24.7 mA per day. The phototransistors charge the capacitors in two seconds, so the energy employed was relatively low and was not included in **Table 3**.

### 3.3.1 Node costs

The costs per hectare for both sensors, together with its WSN network, change. The cheaper system will use V1.2 probes with the BLE CC2541 communication net (1760 US). If ten TTGO LoRa32 OLED V2.1.6 modules are needed to transmit data from 1 ha to the farmer's house, the final cost for all the intelligent systems will be 2200 US\$. In the case of using the laser WSN (option B) with the V1.2 probes and the LoRa modules, the total cost increases to 2950 US\$. Laser WSN using sprinkler-encoder sensors and LoRa will increase the cost to 5100 US\$, meanwhile the sprinkler encoder sensors plus BLE WSN and LoRa will cost 4350 US\$.

### 3.4 UAV images and NDVI

UAV images were taken at midday on April 3rd, 6th, and 9th at three different zones of the plantation. Many trees in the multispectral images (19 + 10) had null NDVI changes after 1 week. In the 19 trees, irrigation was maintained and the other 10 marked with a blue cross (**Figure 9b**) had only one sprinkler removed. After 1 week, those trees without irrigation showed NDVI changes (**Figure 11a** and **b**). Trees grown in loam soil are marked with circles filled with white, being more stressed than those grown over clay soil (red circles). After calculating the NDVI index, trees in loam soil decrease their value from 0.85 to 0.82, as schemed by the blue columns (**Figure 11b**), even when only one sprinkler was removed. The NDVI index of trees standing on clay soil had no variation during the first 4 days when the four sprinklers were removed as shown by the brown column in **Figure 11b**. After 7 days, NDVI index of trees grown on clay soil decreased to 0.81.

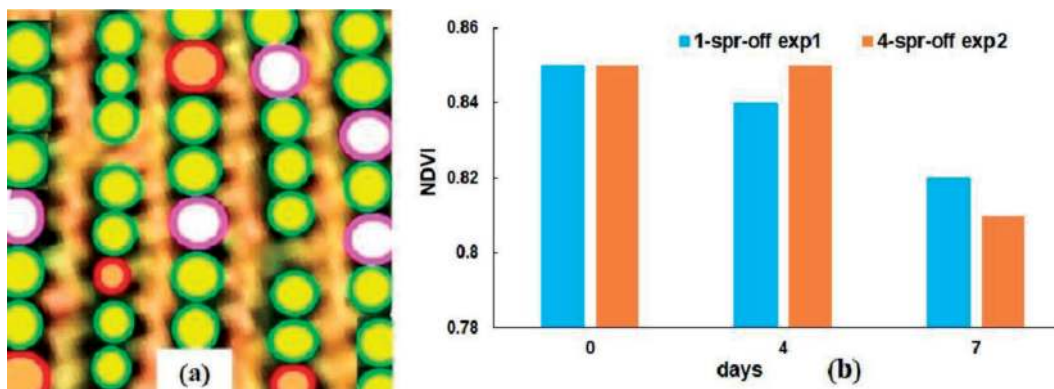


**Figure 11.** UAV tree (a) having some stress, and (b) NDVI during the first, fourth, and seventh day.

#### **4. Conclusions**

Precision agriculture is a technological reality in orchards. In our study, soil sensors resulted in a better option than UAV imaging. UAV platforms require more research and different bands to detect how micro-sprinkler irrigation is working in real-time. Imaging analysis is much more complicated than simple embedded systems and producers. Producers find UAV technology complicated and environmental conditions make them much more difficult to use than simple embedded systems. Imaging analysis obtained by the camera is challenging for them.

Soil moisture sensors in a walnut orchard were tested; some of them as the DHT 11 and YL-69 failed after 1 week of operation. When drops of saturated water pour over the DHT 11 sensor, it failed after 3 days, meanwhile the YL-69 got rusty after applying a direct current voltage to it. The capacitive 1.2 probe covered with a corrosion-resistant material proved to measure properly during several seasons and under clay and loam soil. The V1.2 probe is very cheap and energy-efficient. The sprinkler-decoder sensor was the more efficient sensor based on current consumption, but its price increased by a factor of 2.5. Wetness sensors are being developed with flexible substrates to detect dry and wet conditions but are still very expensive.

WSN groups of nine trees were formed by hectare within the orchard; each group transmitted its information through a LoRa module. The BLE node proved much more economical than the laser system and both operate properly. LoRa modules transmit information toward the farmers' house sending the tree number where the micro-sprinkler failed. LoRa is able to transmit at distances of 500 m even when the temperature ranges between 30 and 35°C. The WSN system can be used to transmit other information from the plantation using a similar version of tree grouping.

#### **Acknowledgements**

We would like to acknowledge Eng. Angel Hernandez, Biol. Ruth Perez for the discussions and to the University Autonoma Chapingo for supporting and funding this project 19008-DTT-65.

## **Author details**

Federico Hahn Schlam<sup>1\*</sup> and Fermín Martínez Solís<sup>2</sup>

1 Irrigation Department, Universidad Autónoma Chapingo, Carretera México-Texcoco, Chapingo, Mexico

2 Engineering Department, Universidad Juárez Autónoma de Tabasco, Tabasco, Mexico

\*Address all correspondence to: fedhahn@gmail.com

## **IntechOpen**

---

© 2022 The Author(s). Licensee IntechOpen. This chapter is distributed under the terms of the Creative Commons Attribution License (<http://creativecommons.org/licenses/by/3.0>), which permits unrestricted use, distribution, and reproduction in any medium, provided the original work is properly cited. 

## References

- [1] Martinez DG, Núñez MH. Current status of pecan production in Mexico and future outlook. In: Proceedings of the 77 Annual Convention of Oklahoma Pecan Growers Association. 2007. 434 pp
- [2] Castillo IO, Sangerman DM, Hernández MF, Vázquez CV, Robles MA. Production and marketing of pecan nuts (*Carya illinoensis* Koch) in northern Coahuila, Mexico. *Revista Mexicana de Ciencias Agrícolas*. 2013;**4**(3):461-476. Corpus ID: 128129723
- [3] Barrett D, Somogyi L, Ramaswamy H. *Processing Fruits*. 2nd ed. Boca Raton, Florida, USA: CRC Press LLC. ISBN: 0-8943-1478-X. 841 pp
- [4] Collin G, Caron J, Létourneau G, Gallichand J. Yield and water use in almond under deficit irrigation. *Agronomy Journal*. 2019;**111**:1381-1391. DOI: 10.2134/agronj2018.03.0183
- [5] INC. International Nut & Dried Fruit. *Nuts & Dried Fruits Statistical Yearbook 2019/2020*. 2019. Available from: <https://www.nutfruit.org/industry/statistics>
- [6] Micke WC, Kester DE. Almond growing in California. *Acta Horticulturae*. 1998;**470**:21-28. DOI: 10.17660/ActaHortic.1998.470.1
- [7] Stevens RM, Ewenz CM, Grigson G, Conner SM. Water use by an irrigated almond orchard. *Irrigation Science*. 2012;**30**(3):189-200. DOI: 10.1007/s00271-011-0270-8
- [8] El-Soda AS, Hend IA, El-Hissen AM, Eid TA. Effect of irrigation levels on growth and productivity of pecan trees. *American-Eurasian Journal of Agricultural & Environmental Sciences*. 2021;**21**(1):60-71. DOI: 10.5829/idosi.aejaes.2021.60.71
- [9] Sánchez JM, Simón L, González-Piqueras J, Montoya F, López-Urrea R. Monitoring crop evapotranspiration and transpiration/evaporation partitioning in a drip-irrigated young almond orchard applying a two-source surface energy balance model. *Water*. 2021;**13**:2073. DOI: 10.3390/w13152073
- [10] Holzapfel EA, Pannunzio A, Lorite I, Oliveira AS, Farkas I. Design and management of irrigation systems. *Chilean Journal of Agricultural Research*. 2009;**69**:17-25. DOI: 10.4067/S0718-58392009000500003
- [11] Ibragimov N, Evett SR, Esanbekov Y, Kamilov BS, Mirzaev L, Lamers JPA. Water use efficiency of irrigated cotton in Uzbekistan under drip and furrow irrigation. *Agricultural Water Management*. 2007;**90**:112-120. DOI: 10.1016/j.agwat.2007.01.016
- [12] Phogat V, Skewes M, Mahadevan M, Cox JW. Seasonal simulation of water and salinity dynamics under different irrigation applications of almond in pulsed and continuous mode. In: 4th International Conference on HYDRUS Software Applications to Subsurface Flow and Contaminant Transport Problems. March 21-23, 2013; Prague, Czech Republic. ISBN: 978-80-213-2368-1
- [13] Shalek Briski A, Brorsen BW, Biermacher JT, Rohla CT, Chaney W. Effect of irrigation method on tree growth, foliar nutrient levels, and nut characteristics of young pecan trees in the southern Great Plains. *HortTechnology*. 2019;**29**(2):109-113. DOI: 10.21273/HORTTECH04162-18
- [14] Girona J, Mata M, Marsal J. Regulated deficit irrigation during the

- kernel-filling period and optimal irrigation rates in almond. *Agricultural Water Management*. 2005;**75**:152-167. DOI: 10.1016/j.agwat.2004.12.008
- [15] Goldhamer DA, Viveros M, Salinas M. Regulated deficit irrigation in almonds: Effects of variations in applied water and stress timing on yield and yield components. *Irrigation Science*. 2006;**24**:101-114. DOI: 10.1007/s00271-005-0014-8
- [16] Zarco-Tejada PJ, Gonzalez-Dugo V, Berni J. Fluorescence, temperature and narrow-band indices acquired from a UAV platform for water stress detection using a micro-hyperspectral imager and a thermal camera. *Remote Sensing of Environment*. 2012;**117**:322-337. DOI: 10.1016/j.rse. 2011.10.007
- [17] Lloret J, Sendra S, Garcia L, Jimenez JM. A wireless sensor network deployment for soil moisture monitoring in precision agriculture. *Sensors*. 2012;**21**:7243. DOI: 10.3390/s21217243
- [18] Shock CC, Wang FY. Soil water tension, a powerful measurement for productivity and stewardship. *HortScience*. 2011;**46**(2):178-185. DOI: 10.21273/HORTSCI.46.2.178
- [19] Jones HG. Irrigation scheduling: Advantages and pitfalls of plant based methods. *Journal of Experimental Botany*. 2004;**55**(407):2427-2436. DOI: 10.1093/jxb/ erh213
- [20] Fereres E, Goldhamer DA. Suitability of stem diameter variations and water potential as indicators for irrigation scheduling of almond trees. *Journal of Horticultural Science and Biotechnology*. 2003;**78**(2):139-144. DOI: 10.1080/14620316.2003.11511596
- [21] Azevedo JA, Santos FE. An empirical propagation model for forest environments at tree trunk level. *IEEE Transactions on Antennas and Propagation*. 2011;**59**(6):2357-2367. DOI: 10.1109/TAP.2011.2143664
- [22] Meng Y, Lee YH, Ng BC. Empirical near ground path loss modeling in a forest at VHF and UHF bands. *IEEE Transactions on Antennas and Propagation*. 2009;**57**(5):1461-1468. DOI: 10.1109/TAP.2009.2016703
- [23] Wiyadi E, Setiadi R, Umar L. Effect of vegetation profile and air data rate on packet loss performance of LoRa E32-30dBm 433 MHz as a wireless data transmission. *Journal of Physics: Conference Series*. 2020;**1655**:012015. DOI: 10.1088/1742-6596/1655/1/012015
- [24] Rizman ZI, Jusoff K, Rais SS, Bakar HH, Nair G, Ho YK. Microwave signal propagation on oil palm trees: Measurements and analysis. *International Journal on Smart Sensing and Intelligent Systems*. 2011;**4**(3):388-401. DOI: 10.21307/IJSSIS-2017-446
- [25] Elijah O, Abdul Rahim S, Sittakul V, Al-Samman A, Cheffena M, Din J, et al. Effect of weather condition on LoRa IoT communication technology in a tropical region: Malaysia. *IEEE Access*. 2021;**9**:72835-72843. DOI: 10.1109/ACCESS.2021.3080317
- [26] Bezerra NS, Åhlund C, Saguna S, Sousa VA. Temperature impact in LoRaWAN—A case study in northern Sweden. *Sensors*. 2019;**19**(20):4414. DOI: 10.3390/s19204414
- [27] Anzum R. Factors that affect LoRa propagation in foliage medium. *Procedia Computer Science*. 2021;**194**:149-155. DOI: 10.1016/j.procs.2021.10.068
- [28] Fang SH, Cheng YC, Chien YR. Exploiting sensed radio strength and precipitation for improved distance

- estimation. *IEEE Sensors Journal*. 2018;**18**(16):6863-6873. DOI: 10.1109/JSEN.2018.2851149
- [29] Zhang C, Valente J, Kooistra L, Guo L, Wang W. Orchard management with small unmanned aerial vehicles: A survey of sensing and analysis approaches. *Precision Agriculture*. 2021;**22**:2007-2052. DOI: 10.1007/s11119-021-09813-y
- [30] Wu Y, Guo G, Tian G, Liu W. A Model with leaf area index and trunk diameter for LoRaWAN radio propagation in Eastern China Mixed Forest. *Journal of Sensors*. 2020; Article ID 2687148. pp. 1-16. DOI: 10.1155/2020/2687148
- [31] Bendig J, Bolten A, Bareth G. Introducing a low-cost mini-UAV for thermal and multispectral imaging. *The International Archives of the Photogrammetry, Remote Sensing and Spatial Information Sciences*. 2012;**39**:345-349. DOI: 10.5194/isprsarchives-XXXIX-B1-345-2012
- [32] Bulanon DM, Lonai J, Skovgard H, Fallahi E. Evaluation of different irrigation methods for an apple orchard using an aerial imaging system. *ISPRS International Journal of Geo-Information*. 2016;**5**(6):79. DOI: 10.3390/ijgi5060079
- [33] Calera A, Campos I, Osann A, D'Urso G, Menenti M. Remote sensing for crop water management: From ET modelling to services for the end users. *Sensors*. 2017;**17**:1104. DOI: 10.3390/s17051104
- [34] Houborg R, Boegh E. Mapping leaf chlorophyll and leaf area index using inverse and forward canopy reflectance modeling and SPOT reflectance data. *Remote Sensing of Environment*. 2008;**112**:186-202. DOI: 10.1016/J.RSE.2007.04.012
- [35] Othman Y, Steele C, VanLeeuwen D, Heerema R, Bawazir A, St. Hilaire R. Remote sensing used to detect moisture status of pecan orchards grown in a desert environment. *International Journal of Remote Sensing*. 2014;**35**:949-966. DOI: 10.1080/01431161.2013.873834
- [36] De Leijster V, Verburg RW, Santos MJ, Wassen MJ, Martínez-Mena M, de Vente J, et al. Almond farm profitability under agroecological management in South-Eastern Spain: Accounting for externalities and opportunity costs. *Agricultural Systems*. 2020;**183**:102878. DOI: 10.1016/j.agsy.2020.102878
- [37] Casanova-Gascón J, Figueras-Panillo M, Iglesias-Castellarnau I, Martín-Ramos P. Comparison of SHD and open-center training systems in almond tree orchards cv. 'Soleta'. *Agronomy*. 2019;**9**:874. DOI: 10.3390/agronomy9120874
- [38] Tarango-Rivero H. Manejo del nogal pecanero con base en su fenología. [Pecan orchard management based in its phenology]. Folleto Técnico 24, Campo Experimental Delicias. 3a ed. Chihuahua: INIFAP; 2012. 39 pp. ISBN: 978-607-425-769-4
- [39] Andersen PC, Crocker TE. The pecan tree: HS984/HS229, 5/2004. 1st ed. Florida Cooperative Extension Service, Institute of Food and Agricultural Sciences, University of Florida; 2004. HS984. DOI: 10.32473/edis-hs229-2004
- [40] Yu L, Tao S, Ren Y, Gao W, Liu X, Hu Y, et al. Comprehensive evaluation of soil moisture sensing technology applications based on analytic hierarchy process and Delphi. *Agriculture*. 2021;**11**:1116. DOI: 10.3390/agriculture11111116
- [41] Kojima Y, Shigeta R, Miyamoto N, Shirahama Y, Nishioka K, Mizoguchi M,

- et al. Low-cost soil moisture profile probe using thin-film capacitors and a capacitive touch sensor. *Sensors*. 2016;**16**(8):1292. DOI: 10.3390/s16081292
- [42] Payero JO, Qiao X, Khalilian A, Mirzakhani-Nafchi A, Davis R. Evaluating the effect of soil texture on the response of three types of sensors used to monitor soil water status. *Journal of Water Resource and Protection*. 2017;**9**:566-577. DOI: 10.4236/jwarpp.2017.96037
- [43] Huang Q, Akinremi OO, Sri Rajan R, Bullock P. Laboratory and field evaluation of five soil water sensors. *Canadian Journal of Soil Science*. 2004;**84**:431-438. DOI: 10.4141/S03-097
- [44] Fauziyah M, Safitri H, Dewatama D, Aulianta E. Conditioning of temperature and soil moisture in chrysanthemum cut flowers greenhouse prototype based on internet of things (IoT). *ELKHA: Journal Teknik Elektro*. 2021;**13**(1):25-32. DOI: 10.26418/elkha.v13i1.43078
- [45] Sudha LK, Sinha A. Effect of moisture content in the sandy, clay and loamy soil using humidity sensor YL 69. *International Journal of Science and Research (IJSR)*. 2017;**6**(5):107-109. Corpus ID: 53474495
- [46] Ihuoma SO, Madramootoo CA. Recent advances in crop water stress detection. *Computers and Electronics in Agriculture*. 2017;**141**:267-275. DOI: 10.1016/j.compag.2017.07.026
- [47] Marakkala Manage LP, Humlekrog Greve M, Knadel M, Moldrup P, De Jonge LW, Katuwal S. Visible-near-infrared spectroscopy prediction of soil characteristics as affected by soil-water content. *Soil Science Society of America Journal*. 2018;**82**:1333-1346. DOI: 10.2136/sssaj2018.01.0052
- [48] Hardie M. Review of novel and emerging proximal soil moisture sensors for use in agriculture. *Sensors*. 2020;**20**:6934. DOI: 10.3390/s20236934
- [49] Bellvert J, Adeline K, Baram S, Pierce L, Sanden BL, Smart DR. Monitoring crop evapotranspiration and crop coefficients over an almond and pistachio orchard throughout remote sensing. *Remote Sensing*. 2018;**10**:2001. DOI: 10.3390/rs10122001
- [50] Machwitz M, Pieruschka R, Berger K, Schlerf M, Aasen H, Fahrner S, et al. Bridging the gap between remote sensing and plant phenotyping—Challenges and opportunities for the next generation of sustainable agriculture. *Frontiers in Plant Science*. 2021;**12**:749374. DOI: 10.3389/fpls.2021.749374
- [51] Rocha J, Perdiao A, Melo R, Henriques C. Remote sensing based crop coefficients for water management in agriculture. In: Curkovic S, editor. *Sustainable Development—Authoritative and Leading Edge Content for Environmental Management*. London, UK: IntechOpen Limited; 2012. pp. 167-191. Chapter 8
- [52] González-Dugo V, Zarco-Tejada PJ, Fereres E. Applicability and limitations of using the crop water stress index as an indicator of water deficits in citrus orchards. *Agricultural and Forest Meteorology*. 2014;**198-199**:94-104. DOI: 10.1016/j.agrformet.2014.08.003
- [53] Wong CYS, Bambach NE, Alsina MM, McElrone AJ, Jones T, Buckley TN, et al. Detecting short-term stress and recovery events in a vineyard using tower-based remote sensing of photochemical reflectance index (PRI). *Irrigation Science*. 2022;**40**(3). DOI: 10.1007/s00271-022-00777-z
- [54] Jafarbiglu H, Pourreza A. A comprehensive review of remote sensing

platforms, sensors, and applications in nut crops. *Computers and Electronics in Agriculture*. 2022;**197**:106844. DOI: 10.1016/j.compag.2022.106844

[55] Teixeira AA, Mendes J, Cláudio W, Bredemeier C, Negreiros M, Aquino R. Evaluation of the radiometric accuracy of images obtained by a sequoia multispectral camera. *Engenharia Agrícola*. 2020;**40**(6):759-768. DOI: 10.1590/1809-4430-Eng.Agric.v40n6p759-768/2020

[56] Candiago S, Remondino F, De Giglio M, Dubbini M, Gattelli M. Evaluating multispectral images and vegetation indices for precision farming applications from UAV images. *Remote Sensing*. 2015;**7**:4026-4047. DOI: 10.3390/rs70404026

[57] Adla S, Rai NK, Karumanchi SH, Tripathi S, Disse M, Pande S. Laboratory calibration and performance evaluation of low-cost capacitive and very low-cost resistive soil moisture sensors. *Sensors*. 2020;**20**:363. DOI: 10.3390/s20020363

[58] Bouyoucos GJ, Mick AH. A comparison of electric resistance units for making a continuous measurement of soil moisture under field conditions. *Plant Physiology*. 1948;**23**(4):532-543. DOI: 10.1104/pp.23.4.532

[59] Huang SC, Lin YZ. A low-cost constant-moisture automatic irrigation system using dynamic irrigation interval adjustment. *Applied Science*. 2020;**10**:6352. DOI: 10.3390/app10186352

[60] Sentelhas PC, Monteiro JE, Gillespie TJ. Electronic leaf wetness duration sensor: Why it should be painted. *International Journal of Biometeorology*. 2004;**48**(4):202-205. DOI: 10.1007/s00484-004-0200-z

[61] Patle KS, Saini R, Kumar A, Surya SG, Palaparthi VS, Salama KN. IoT enabled, leaf wetness sensor on the flexible substrates for in-situ plant disease management. *IEEE Sensors Journal*. 2021:1-1. DOI: 10.1109/jsen.2021.3089722